Rock Mechanics Bulletin 4 (2025) 100193

Full Length Article

The effect of geometrical parameters on wedge failure of rock slopes using physical and numerical modelling

Mohammadmatin Mahdizadeh [a], Erfan Amini [a], Mohammad Hossein Khosravi [b,*]

[a] School of Mining Engineering, College of Engineering, University of Tehran, Tehran, Iran
[b] Department of Mining Engineering, Faculty of Engineering, University of Birjand, Birjand, Iran

ARTICLE INFO

Keywords:
Rock slope stability
Wedge failure
Wedge factor
Physical modeling
Numerical modeling

ABSTRACT

This study investigated the role of the geometrical parameters of a wedge block on its stability using physical and numerical modeling. For the purpose of physical modeling, a new experimental setup was developed, and the stability of rock slopes was modeled. Sensitivity analysis was performed on four geometrical parameters: tilt angle of the wedge (β), included angle of the wedge (ξ), the apparent dip of the slope in the sliding direction (Ψ_{fi}), and the difference in dip direction of the slope face and discontinuities intersection line ($\Delta\alpha$). A total number of 89 rock slope models were tested, and the wedge factor (K) was calculated for each model. Subsequently, 3D numerical models, corresponding to each physical model were conducted. Rock slope face inclination was applied by defining gravity vectors in different directions, which led to the development of models with a much simpler geometry. Ultimately, numerical modeling results almost align with the outcomes of physical modeling. Good agreement was observed between physical and numerical models and the existing analysis. According to the results, the behavior of the wedge-shaped block and its safety factor depends on the geometric conditions of the wedge and its slope, regardless of the rock material properties, as models were tested with two different materials. Additionally, sensitivity analysis demonstrates that by increasing $\Delta\alpha$, the slope safety factor was increased, as expected. Finally, practical graphs were developed by which the safety factor against the wedge failure can be estimated using the geometrical parameters of the wedge and the rock slope.

1. Introduction

One of the main and classical problems in geotechnical engineering is to evaluate and maintain the stability of natural and man-made rock slopes. In plenty of civil projects such as highways, dams, building constructions, and also for mining purposes, especially in open pit mines, these excavated slopes may become unstable and lead to several casualties and economic consequences (Kumsar et al., 2000; Yang et al., 2024). Therefore, in many geotechnical and mining projects, slope stability analysis is an essential requirement. A failure in a soil/rock slope is caused by the predominance of driving forces over resistance forces. The factor of safety is a common parameter in the design of slopes and considering its uncertainties (Wu et al., 2023). Many parameters such as geological and lithological conditions of the slope, the slope's specific geometry, the state of joint sets, dimensions of the rock slope, ground and underground water conditions, and earthquakes are leading to different types of soil/rock slope failures (Amini et al., 2023; Bowa, 2020; Jaiswal et al., 2024; Mahmoodzadeh et al., 2023). In general, plane failure, wedge failure, toppling failure, circular failure, and in some cases a combination of different failure types could happen in rock slopes (Wyllie and Mah, 2004). There are various methods to identify the probable modes of failure and analyze the stability of slopes, such as kinematic analysis, analytical approaches, and numerical and physical modelings. Kinematic analysis is a simple and practical way to identify the probable modes of failure, and deterministic kinematic analysis can be done with a classical method called stereographic projection technique (Zheng et al., 2016). As a result, numerous researchers such as Goodman (1976), Hoek and Bray (1981), and Yoon et al. (2002) had utilized this technique. Limit analysis is another method of kinematical analysis and Li et al. (2023) have utilized upper-bound limit analysis for slope stability. The limit equilibrium technique is classified as an analytical approach. Simplified Bishop and modified Bishop, Fellenius, Janbu, Spencer, Morgenstern-Price, Swedish circle, and Sarma are among the most common limit equilibrium

https://doi.org/10.1016/j.rockmb.2025.100193
Received 7 August 2024; Received in revised form 19 November 2024; Accepted 20 February 2025
Available online 20 March 2025

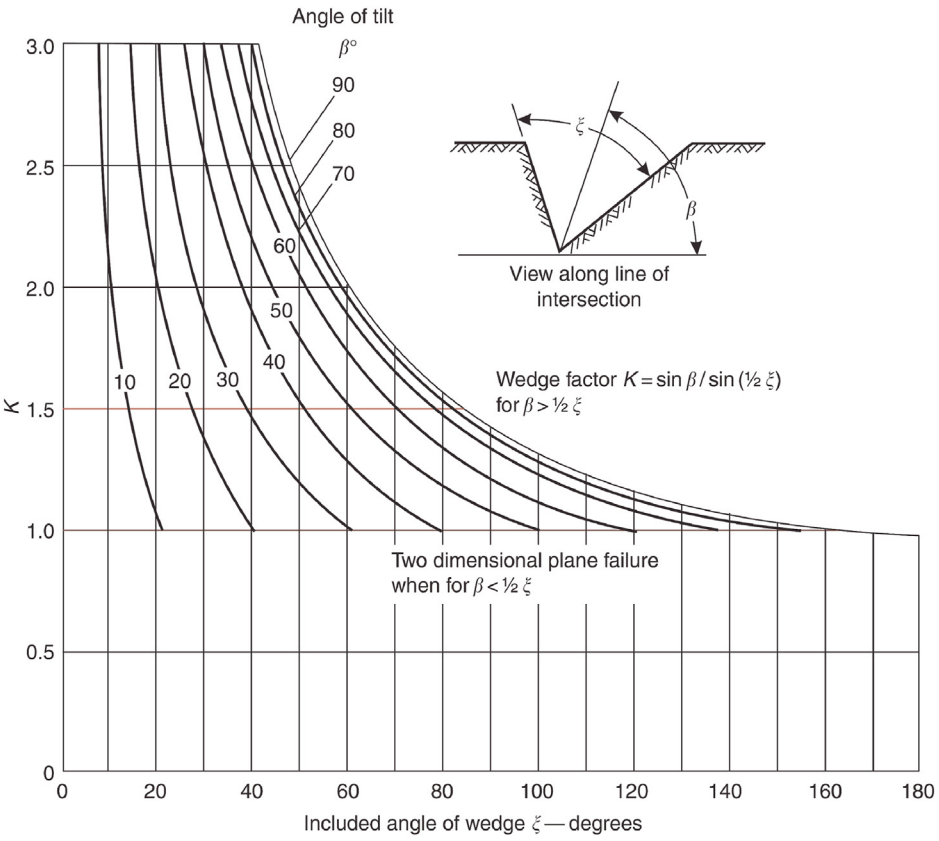

Fig. 1. Wedge factor illustrated as a function of wedge geometrical properties (Wyllie and Mah, 2004).

techniques (Ahmed et al., 2012; Alfat et al., 2019; Hazari et al., 2020; Jiang and Yamagami, 2004; Kumar et al., 2024; Prabowo et al., 2024; Sarfaraz et al., 2023b; Sheng et al., 2021). Numerical simulation of slope stability analysis could be modeled in both continuum or discontinuum environment (Wang et al., 2012, 2014). Stability analysis of slopes can be modeled physically using a tilting table or centrifuge (Amini et al., 2015; Ling et al., 2009). It is worth to be mentioned that, the above-mentioned methods can be coupled with each other (Singh et al., 2024).

Wedge failure is a type of failure that occurs specifically in rock slopes with two sets of intersecting joint sets (Hoek et al., 1973). Based on the placement of the two joint sets and consequently formation of tetrahedral wedges, three different modes of failure may occur: sliding along the intersection line, sliding along joint one, sliding along joint two (Jiang et al., 2013; Lucas, 1980; Zheng et al., 2016). In some cases, there is a possibility that the joint sets will not form any wedges (Zheng et al., 2016). The mechanism of this failure and the contributing factors in estimating the factor of safety is one of the rock mechanics and geotechnical engineers' goals.

The wedge failure has been investigated by some researchers over the years, and the modes of failure were differentiated by them (Chen, 2004; Goodman, 1976; Hoek and Bray, 1981; Lucas, 1980). In addition, several previous analytical studies on wedge failure mechanism have been done mainly by Wittke (1965), John (1970), Hoek et al. (1973), Kovári and Fritz (1975), and Hoek and Bray (1981); in this regard, physical experiments also have been done by researchers such as Kumsar et al. (2000). Other researchers such as Zheng et al., (2016, 2017) developed a probabilistic kinematic analysis for analyzing the procedure of wedge failure and its applicability in engineering projects like an open pit mine or a hydropower site. Hoek et al. (1973) presented a preliminary graph for calculating the wedge failure factor of safety for cohesionless planes. According to this analysis, the safety factor of a wedge block depends on three slope geometrical parameters: the tilt angle of the wedge (β), the included angle of the wedge (ξ), and the apparent dip of the slope in the sliding direction (Ψ_{fi}).

According to Wyllie and Mah (2004), the initial condition for sliding a rock wedge, developed by cohesionless discontinuities, is as follows:

$$\phi < \psi_i < \psi_{fi} \tag{1}$$

where ψ_{fi} is the apparent dip of the slope in the sliding direction, ψ_i is the dip angle of the discontinuities' intersection lines, and ϕ is the friction angle of the discontinuities. Based on this analysis, if the intersecting discontinuities have the same friction, the safety factor of the wedge (FS_W) can be calculated as a ratio of the safety factor of a cohesionless plane (FS_P) under the same condition.

$$FS_W = K \cdot FS_P \tag{2}$$

$$FS_P = \frac{\tan \phi}{\tan \psi_i} \tag{3}$$

$$K = \frac{\sin \beta}{\sin\left(\frac{\xi}{2}\right)} \tag{4}$$

where K is the wedge factor, ϕ is the friction angle of the discontinuities, ψ_i is the dip angle of the discontinuities' intersection line, β is the tilt angle of the wedge and ξ is the included angle of the wedge. The wedge factor, as a function of the wedge geometrical properties, is illustrated in Fig. 1.

As stated above, the Hoek et al. (1973) approach has some limitations in use. For instance, the planes must be cohesionless and the friction angle of the planes must be the same. Jiang et al. (2013) solve these curbs by introducing a new method for obtaining the effective normal forces

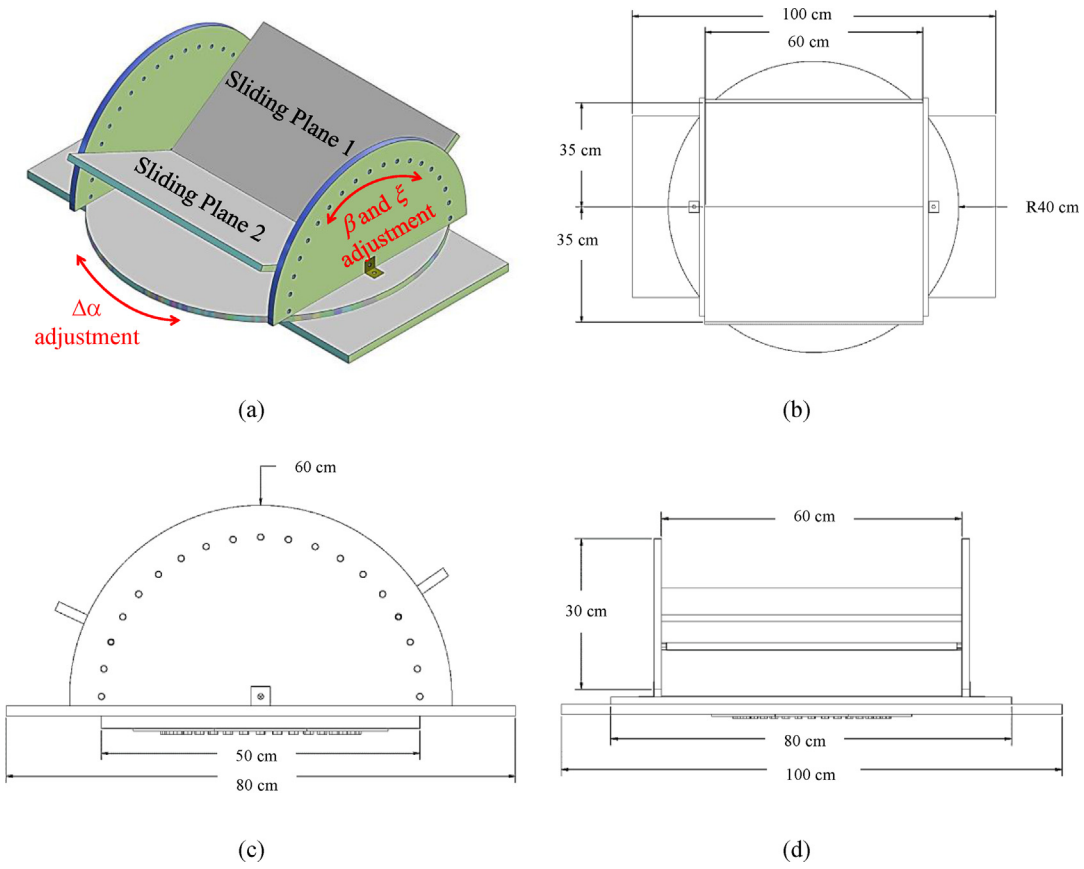

Fig. 2. Experimental setup dimension plan; (a) Isometric view, (b) Top view, (c) Front view, (d) Side view.

acting on the plane in analyzing the stability of rock wedges. Moreover, previous methods mostly discuss the effect of the apparent dip of the slope in the sliding direction. However, the effect of the angle difference between the direction of the slope face and the orientation of the intersection line of the discontinuities, defined as $\Delta\alpha$, can play a significant role in accurately determining the wedge's failure mode and its safety factor.

This paper aims to study the effect of the slope geometrical parameters, the mentioned wedge factor, and $\Delta\alpha$ angle, on the slope stability and behavior.

The investigation procedure in this study included three parts. The first part was to find appropriate material for constructing physical models, with the ability to provide the specific required properties. The second part was to design and construct a testing setup, based on variable parameters. The last part was conducting a series of physical and numerical models with a variation of wedge and slope geometrical parameters. Each part of the investigation is presented in the following sections.

2. Physical modeling

2.1. Material properties

Using the appropriate materials in physical modeling is an essential asset for having a reliable result. In this study, friction powder and Firuzkuh silica sand were used to model wedges in different geometric conditions.

The friction powder is a white laboratory material that is commonly used to build and model blocks with specific geotechnical specifications. This powder consists of $BaSO_4$, ZnO, clay, fine sand, gypsum, and Vaseline, which forms a uniform block with specific properties under a certain amount of pressure (Amini et al., 2017, 2018).

In order to study the effect of the geometrical parameters on the wedge stability, the strength properties of the discontinuities must be unchanged throughout the tests. As this study was limited to cohesionless discontinuities, according to Eqs. (2)–(4), the friction angle of the discontinuities is the only strength property that plays a role in the stability. The friction angle is itself a function of the block density, so the density of the wedge block must be constant in all the tests. In these experiments, powder blocks were modeled with a bulk density of $\rho = 2500$ kg/m^3. The interface friction angle between the wedge block and modeling setup's plates, simulating the discontinuities, was measured equal to 35° through some slip tests.

Silica sand is known as a standard soil and its use in geotechnical research is very common (Ahmadi et al., 2018; Khosravi et al., 2011; Moussaei et al., 2019; Sabermahani et al., 2009). Therefore, as an alternative modeling material, Firuzkuh silica sand with a bulk density of $\rho = 1400$ kg/m^3, a water content of $\omega = 10$ %, and an interface friction angle of $\phi = 28^o$ was used in this study. Note that the apparent interface cohesion due to capillary force was ignorable and is not considered in this study.

2.2. Experimental setup

According to the basic analysis of the wedge failure discussed previously, the modeling setup should have the ability to model various geometrical wedge parameters such as β, ξ, ψ_{fi}, and $\Delta\alpha$. In this regard, a new movable experimental setup was designed and combined with an existing tilting table in the Laboratory of Rock Mechanics of the University of Tehran. Using the tilting technique for laboratory-scale physical modeling of slopes is very common in geotechnical engineering (Alejano et al., 2012; Amini et al., 2017; Khorasani et al., 2019; Kim et al., 2016; Kumsar et al., 2000; Rabat et al., 2022; Sarfaraz et al., 2023a).

The modeling setup was designed in SOLIDWORKS software (BIOVIA,

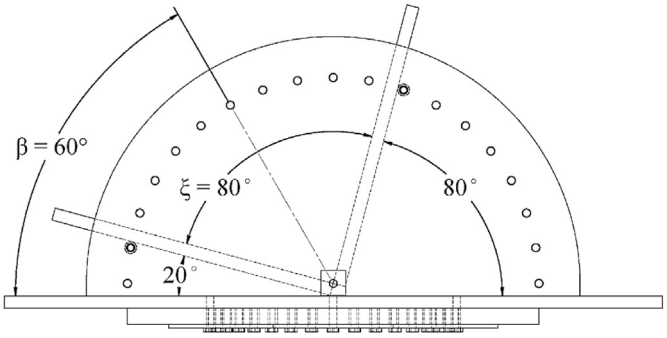

Fig. 3. A wedge with $\xi = 80°$ and $\beta = 60°$ resulted from intersecting two discontinuity planes with dips of 20° and 80°.

2023), as illustrated in Fig. 2. In order to install on the tilting table, the setup consisted of a rectangular chassis. To provide a wide range of ξ and β angles, two semicircular parts create a graded frame at 10-degree intervals, which are assembled and secured with rods and bolts. The two main discontinuity plates, which are completely the same, smooth and polished wooden plates forming the wedge, are installed in the graded frame in specific calculated and required degrees to create particular geometrical conditions of the wedge in each test. In addition, to investigate the effect of $\Delta\alpha$ on the slope stability, the entire frame of the wedge block model was installed on a rotating circle-shaped base, that can create the $\Delta\alpha$ angle in the range of 360° with 10° intervals.

A wide variety of rock wedges resulting from the intersection of two discontinuities can be modeled by the developed experimental setup. As an example, Fig. 3 illustrates the intersection of two discontinuities with dips of 20° and 80°. As can be seen from the figure, it shapes a wedge with the included angle of $\xi = 80°$ and tilt angle of $\beta = 60°$.

The modeling setup was placed on the tilting table as shown in Fig. 4. The used tilting table consists of a box-shaped structure of 100 cm × 50 cm × 70 cm, with the ability to rotate around a horizontal axis and provide a maximum inclination of 40°, using an electrical motor. In order to avoid unwanted dynamic effects in the model inside the box, the table rotation rate was limited to one degree per minute.

2.3. Model preparation

The quality of the model preparation greatly affects the modeling results (Vaneghi et al., 2021), therefore, the initial step for creating a wedge model was to adjust the setup in the desired geometrical angles of ξ, β, Ψ_{fi}, and $\Delta\alpha$, for each test. In order to prepare a wedge block with a uniform target density of $\rho = 1400$ kg/m^3, it was necessary to calculate the volume of the target wedge in each model. Then by controlling the required soil mass, the target density could be reached. By knowing the included angle of the wedge (ξ), the width of the wedge on each discontinuity plane (W), and the length of the wedge (L), the volume of the wedge (V_w) was calculated by Eq. (5).

$$V_W = \frac{1}{2}W^2 L \sin\xi \tag{5}$$

A symmetric block prepared inside the setup is illustrated in Fig. 5.

2.4. Methodology

In general, each test is done in four main stages.

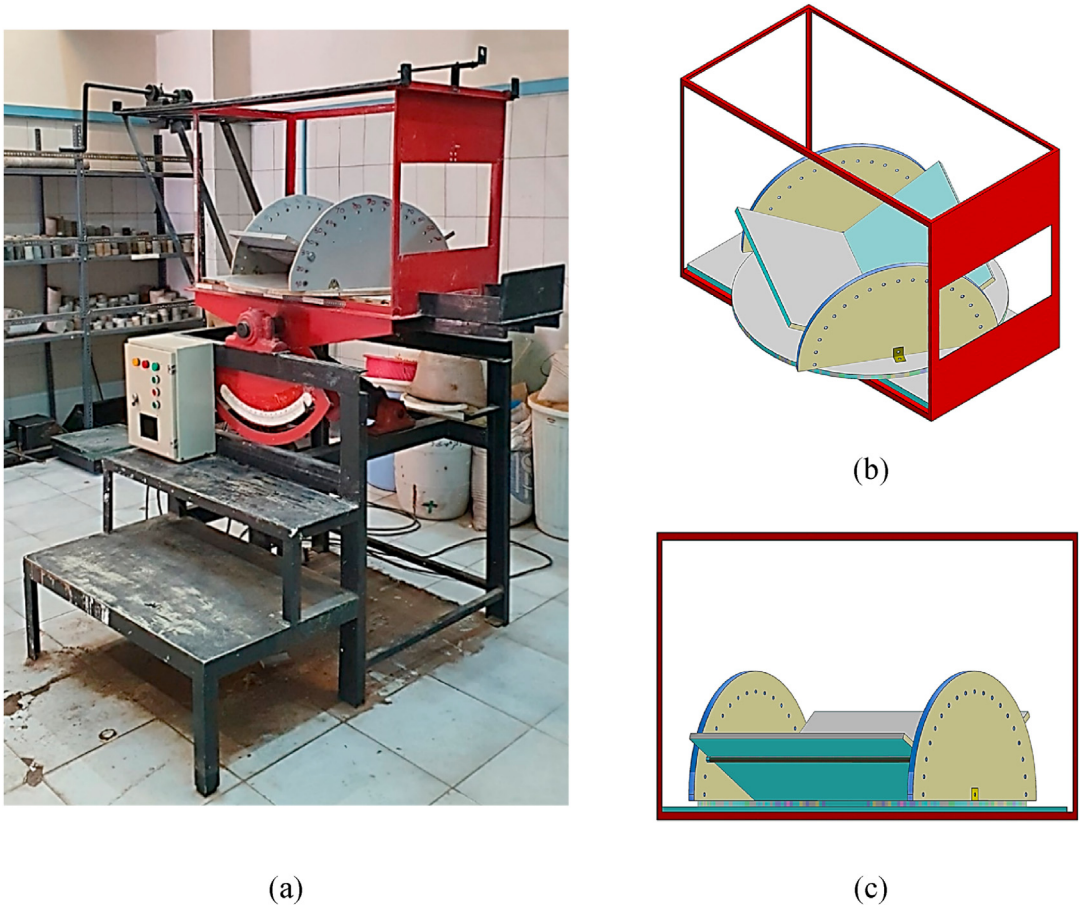

Fig. 4. Physical modeling setup; (a) Setup installed on the tilting table, (b) Isometric view, (c) Side view.

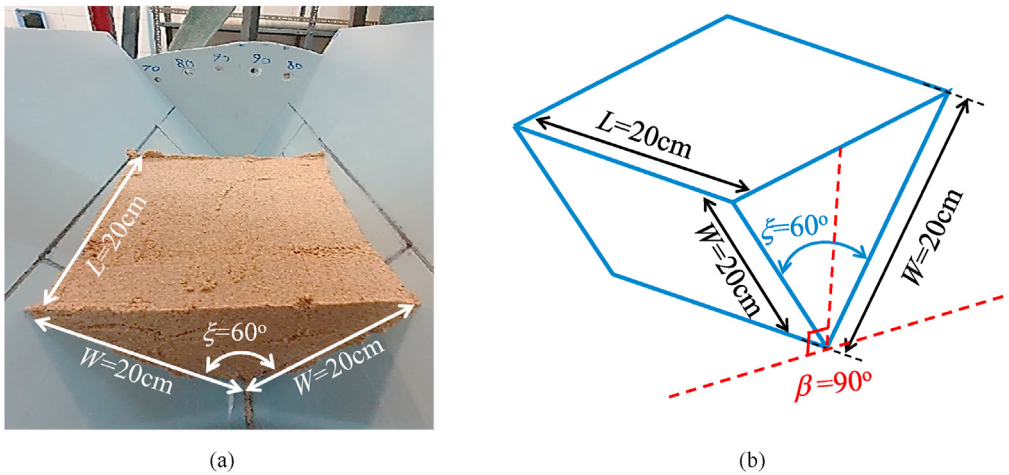

Fig. 5. A symmetric wedge block with $L = W = 20$ cm, $\beta = 90°$, $\xi = 60°$; (a) Physical model, (b) Schematization.

Fig. 6. Physical models with $\Delta\alpha \neq 0°$; (a) Models with positive $\Delta\alpha$ ($\beta = 60°$, $\xi = 90°$, $\Delta\alpha = +40°$), (b) Models with negative $\Delta\alpha$ ($\beta = 60°$, $\xi = 90°$, $\Delta\alpha = -40°$).

1. Adjust the modeling setup in the required geometric condition and prepare the mold for making the wedge block sample,
2. Creating the wedge block with specified material (frictional powder or moisture sand),
3. Generating the inclination or slope dip (Ψ_{fi}), using the tilting table apparatus with a rate of one degree per minute until the moment that sliding occurs,
4. At each test, the final inclination angle of the table and slope, which is practically the dip of the intersection line between two discontinuity planes (Ψ_i), was measured by the apparatus's potentiometer and recorded.

The dip of the discontinuities intersection line (Ψ_{fi}), increases by tilting the table until the moment of the failure. This is also the moment when the block is on the verge of sliding so the factor of safety is equal to one. Eventually, the final value of the angle Ψ_{fi} is recorded. Since the existing tilting table has the ability to create inclinations within 0°–40°, for creating dips higher than 40° in models, an initial dip has been applied to the wedge modeling setup.

In the first series of tests, wedges with different angles of β and ξ were modeled and their corresponding Ψ_{fi} was recorded. In the other series of tests, sensitivity analyses were performed to study the influence of the difference between dip directions of the slope face and discontinuities intersection ($\Delta\alpha$) on the block stability. In the case of inclined wedges ($\beta \neq 90°$), the values of $\Delta\alpha$ have been modeled in two clockwise and counter-clockwise rotations, as demonstrated in Fig. 6. The positive values of $\Delta\alpha$ are considered for clockwise rotations; when the upper discontinuity plane is set through the direction of the tilting table's dip (Ψ_{fi}); and the negative values of $\Delta\alpha$ are considered for the counter-clockwise rotations, which put the underside discontinuity plane through the slope total apparent inclination. In total, 89 tests have been experimented and analyzed in different geometric circumstances.

3. Numerical modeling

The Distinct Element Method (DEM) is a numerical solution introduced by Cundall (1971) and developed to investigate the response of discontinuous media in rock mechanics problems. The DEM is a widely used discontinuum numerical technique to analyze various rock mechanical issues such as brittle failure in rock, fault activation influenced zone and the behavior of rock slopes, generally because of its high capability to model joints (Bonilla-Sierra et al., 2017; Chen et al., 2023; Pradhan and Siddique, 2020; Zhao and Collins, 2024).

Based on a DEM code, a series of numerical models were created corresponding to the physical models. To achieve this, an initial uniform base block was created, then it was cut with the two specific major discontinuity planes, or joint sets, forming the wedge-shaped block. The starting point, orientation, and dip of these planes define the included angle (ξ) and the tilt angle (β) of the wedge for each model, as shown in Fig. 7. The Mohr-Coulomb constitutive model was used where the strength properties of the model were defined similar to those measured in physical modeling. Typical joint shear stiffness (K_s) and joint normal

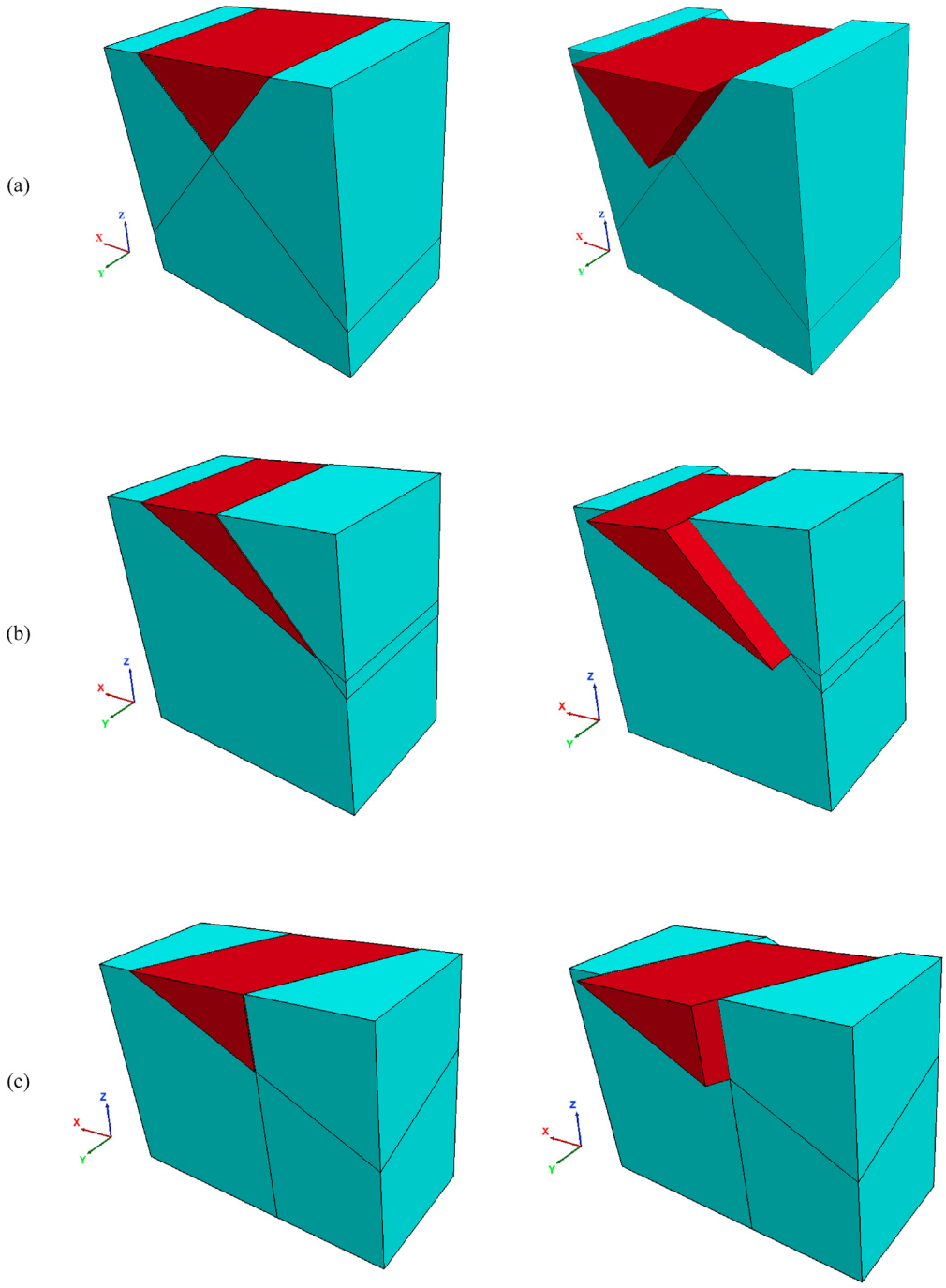

Fig. 7. Numerical model set up before and after the failure; (a) Simple wedge ($\beta = 90°$, $\xi = 90°$, $\Delta\alpha = 0°$), (b) Wedge with overhanging wall ($\beta = 40°$, $\xi = 20°$, $\Delta\alpha = 0°$), (c) Wedge with $\Delta\alpha \neq 0°$ ($\beta = 60°$, $\xi = 60°$, $\Delta\alpha = +30°$).

stiffness (K_n) of 10 MPa/m are assigned to both cohesionless joint sets.

In the numerical setup, the tilting of the model is simulated by rotation of the gravity vector, as illustrated in Fig. 8. Then the components of the gravity vector in three Cartesian directions can be calculated from Eq. (6). Note that the value of g is assumed to be equal to 9.81 m/s^2 in this study.

$$g = (0, g \sin \psi_i, -g \cos \psi_i) \tag{6}$$

The identical methodology was applied to numerical wedge models as in physical models. Accordingly, the slope dip increases by applying different values for the gravity vector until the moment of failure. This is the moment when the block is on the verge of sliding, so the FS is equal to one. In most cases, the stability of the slope is analyzed by observing the behavior of specified points on the model (Bowa and Kasanda, 2020). In this study, the slope crest, on the top of the wedge block formed by joint sets, was monitored, and the program provided the unbalanced force information for this point on the numerical model. Consequently, it demonstrates the moment when the failure occurs, enabling us to record the corresponding slope angle as the result for each distinct geometric condition. Fig. 9 represents the unbalanced force diagram of the slope crest for a model with $\Delta\alpha = 0°$, $\beta = 90°$, and $\xi = 90°$ when the wedge block is on the verge of sliding.

4. Results and discussion

This research was conducted to study the influence of the geometrical

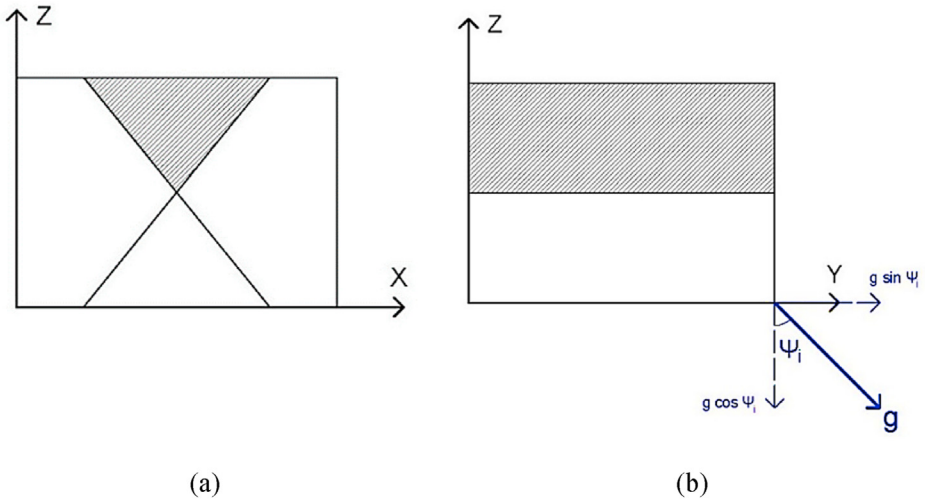

Fig. 8. Simulation of model tilting by rotation of gravity vector in numerical models; (a) Front view, (b) Side view.

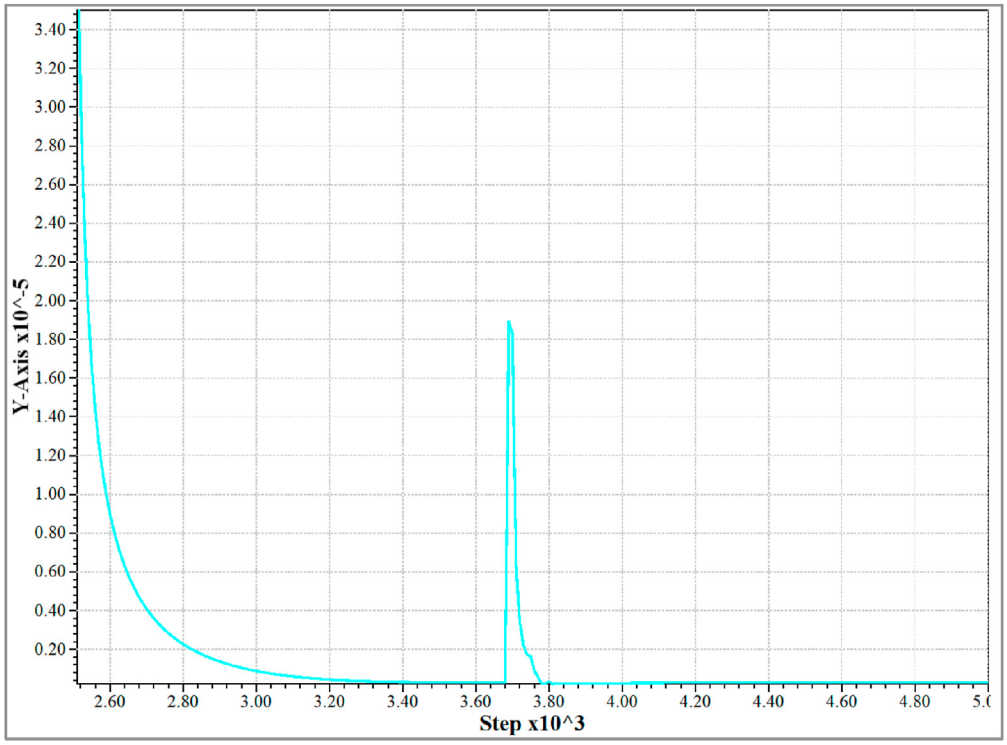

Fig. 9. An example of the maximum unbalanced force of a model on the verge of failure ($\Delta\alpha = 0°$, $\beta = 90°$, and $\xi = 90°$).

parameters of wedge blocks on their stability using physical and numerical modeling. To this end, two series of models were conducted. In the first series, wedges with $\Delta\alpha = 0^0$, β angles of 90°, 60°, 40° and 20°, and ξ angles of 180°, 160°, 140°, 120°, 100°, 90°, 80°, 70°, 60°, 50°, 40°, and 30° were modeled. In the second series, sensitivity analysis was done with the $\Delta\alpha$ angle of 10^0 to 70° for wedges with two β angles of 90° and 60°, and ξ angles of 180°, 150°, 120°, 90°, and 60°. The dip angle of the slope (Ψ_i), was recorded for each model on the verge of failure ($FS = 1$).

4.1. Models with $\Delta\alpha = 0°$

According to Eqs. (2) and (3), at the instant of wedge slippage the safety factor of the wedge is equal to one. Therefore, the wedge factor can be calculated from Eq. (7). This equation was applied to calculate the values of wedge factor in each model.

$$K = \frac{\tan \psi_i}{\tan \phi} \tag{7}$$

The results of physical and numerical models are plotted and compared with the analytical graphs of Hoek et al. (1973) in Fig. 10.

A very good alignment can be seen between the results of physical and numerical models and the analytical predictions of Hoek et al. (1973). Although two different materials were used in the physical models, the results are consistent and follow the same trend. Therefore, it can be concluded that the stability of the wedge does not even depend on its constituent materials and only depends on its geometrical parameters and resistance properties of the discontinuities. According to these results, the wedge factor fluctuates between the values of 1 and about 3, which is consistent with Hoek et al. (1973).

The slight visible difference between the results of physical and

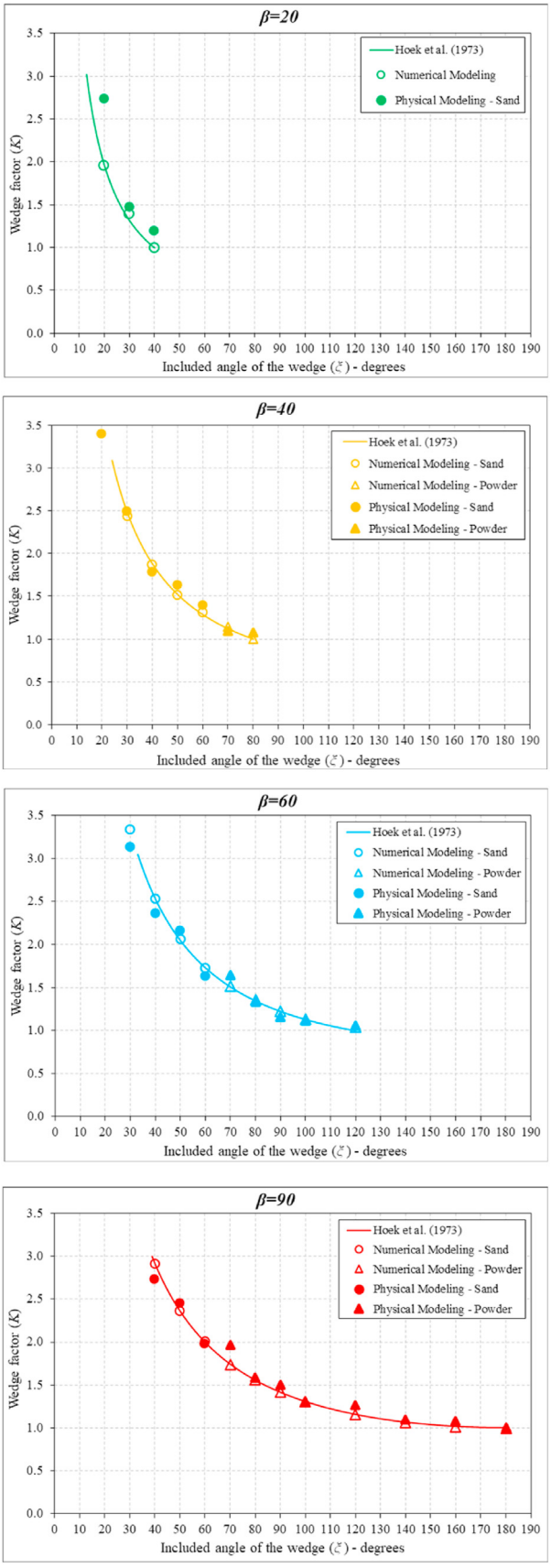

Fig. 10. Comparing physical and numerical results with the analytical graphs of Hoek et al. (1973).

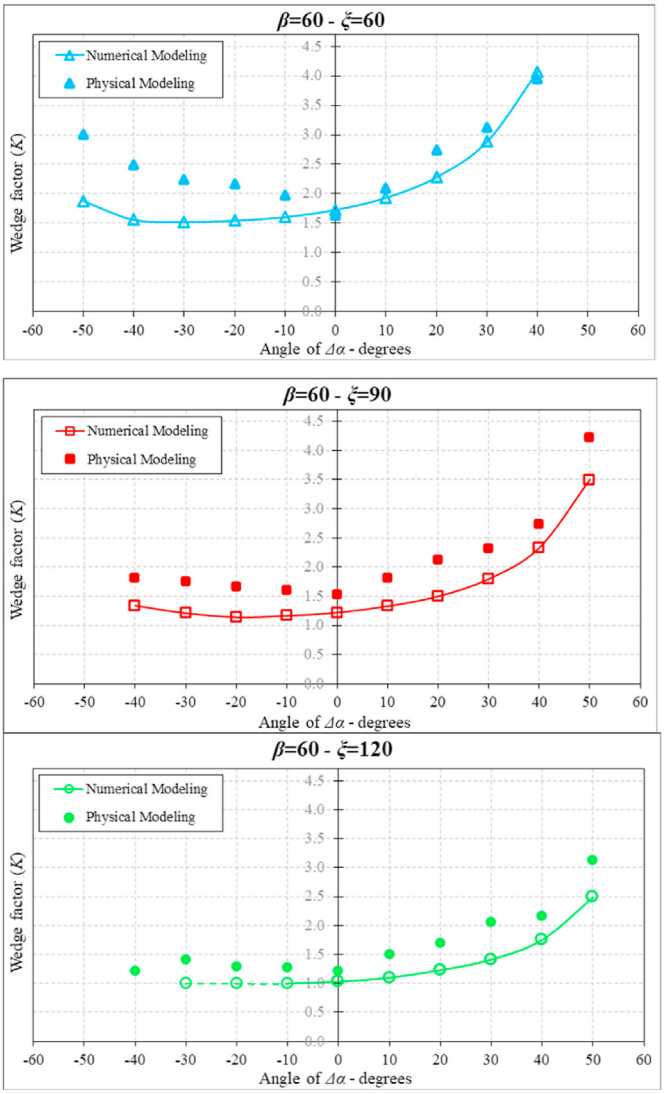

Fig. 11. Comparing physical and numerical results—Models with $\Delta\alpha \neq 0^\circ$ and $\beta = 60^\circ$.

numerical models in Fig. 10, especially at the tilt angle of $\beta = 20^\circ$, is probably due to the adhesion caused by moisture between the block and the discontinuity plates. It should be noted that discontinuity planes were defined as cohesionless in numerical models.

4.2. Models with $\Delta\alpha \neq 0^0$

The previous section was limited to slope models where the wedge angle, intersection line, and the apparent slope face have the same dip direction. To address this missing parameter; this difference in dip directions is defined as $\Delta\alpha$, and sensitivity analysis on its different values was done, and the slope face apparent dip (Ψ^{ft}) has been recorded at the point of failure ($FS = 1$).

To demonstrate, discuss, and analyze the results of these models, the inverse equation of the safety factor in plane failure, which is equivalent to K, and can be defined as a parameter of the FS in wedge failure, was used. Therefore, the inclination of discontinuity planes intersection line (Ψ_i) is independent of the plane faces friction angle (ϕ); which makes it possible to discuss the results regardless of the material used in each test.

To discuss and analyze the results, the value of the aforementioned wedge factor is illustrated in Figs. 11 and 12 as a function of $\Delta\alpha$.

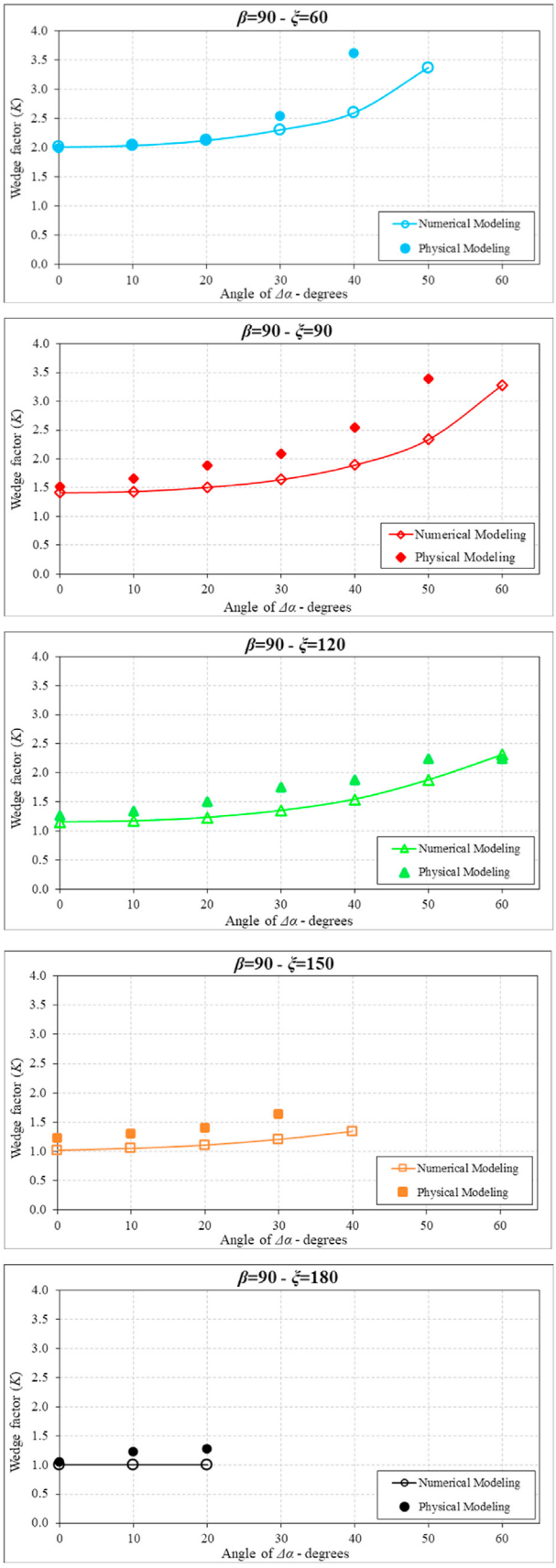

Fig. 12. Comparing physical and numerical results—Models with $\Delta\alpha \neq 0^\circ$ and $\beta = 90^\circ$.

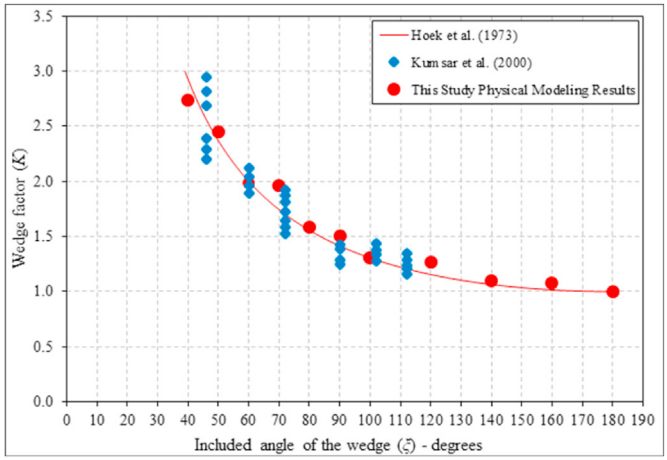

Fig. 13. Comparing physical modeling results with Kumsar et al. (2000) physical models—$\Delta\alpha = 0^\circ$ and $\beta = 90^\circ$.

According to modeling results, the wedge factor increases by increasing $\Delta\alpha$, resulting in a higher safety factor of the block. This trend continues till the point when there is no possibility of failure, or sliding occurs on the lower discontinuity plane. This failure mode happens when one of the discontinuity planes has a dip direction very close to the slope's apparent dip direction. In physical models with $\beta = 60^\circ$, $\xi = 120$, $\Delta\alpha = -40$ and $\beta = 60^\circ$, $\xi = 60$, $\Delta\alpha = -50^\circ$, the sliding is in this failure mode criteria.

Although both physical and numerical analyses suggest almost the same behavior in rock slopes, physical models exhibited greater resistance to failure, especially in models with negative values of $\Delta\alpha$. This effect was particularly pronounced in wedges with smaller opening angles, such as models with $\xi = 60^\circ$. This greater resistance appears to result from the unavoidable cohesion introduced by moisture between the plates and the sliding block.

4.3. Comparison with the results of Kumsar et al. (2000)

Kumsar et al. (2000) modeled wedge failure in rock slopes in a comparable manner, although at a smaller scale. Therefore, concrete wedge blocks were used in six different geometrical conditions with included wedge angles (ξ) of 46°, 60°, 72°, 90°, 102°, and 112°, a tilt angle of $\beta = 90^\circ$, $\Delta\alpha = 0^\circ$, and a friction angle of $\phi = 35^\circ$. Each wedge was modeled several times, and the dip angle of the discontinuities' intersection line (ψ_i) during the failure of each wedge model was measured. To compare the results of Kumsar et al. (2000) with the physical modeling results of this study, based on the values of ψ_i and ϕ, wedge factors (K) were calculated. The results are plotted and compared in Fig. 13. A very good agreement is seen between the results of Kumsar et al. (2000), this study and the theory of Hoek et al. (1973).

5. Conclusions

This research was conducted to discuss the effect of geometrical parameters on wedge failure and evaluate and develop the previous studies by using physical and numerical modeling. An experimental setup was designed and built on a tilting table to model wedge failure in different geometrical states. All the physical and numerical results were demonstrated and compared in graphs based on the defined wedge factor (K) and slope safety factor (FS).

(1) Both physical and numerical results clearly show the accuracy of the analytical graph presented by Hoek et al. (1973). Also, an unequivocal correlation between the safety factor and geometrical

parameters was evident, regardless of the rock slope material properties.

(2) In addition to the parameters studied by Hoek et al. (1973), the influence of the difference angle between the dip directions of the slope face and the discontinuity planes intersection line, shown by $\Delta\alpha$, was studied. Results clearly show that increasing $\Delta\alpha$ resulted in a higher slope safety factor.

(3) The study of the $\Delta\alpha$ angle shows that blocks with specific geometries have the possibility of sliding along only one discontinuity, much like a plane failure. This failure mode occurs if the dip direction of one discontinuity plane is in the same direction as the slope's apparent dip; if the overall slope dip is higher than the friction angle between the faces, the block slides along one discontinuity. According to the results, the safety factor of this planar failure is less than its equivalent wedge failure, which means that the block is more likely to slide under the circumstances of a planar failure mode. This was visibly seen during both physical and numerical models.

(4) Eventually, the graphs in Figs. 11 and 12 developed based on geometrical angles of ξ, β, $\Delta\alpha$, and Ψ_{fi}, and the discontinuities friction angle (ϕ). These graphs can be used in the approximate calculation of wedge failure safety factor, based on the geometrical condition. Notably, since cohesion is inevitable in practical applications, the results of physical modeling provide a more accurate and realistic representation.

CRediT authorship contribution statement

Mohammadmatin Mahdizadeh: Writing – original draft, Validation, Software, Methodology, Formal analysis, Data curation. **Erfan Amini:** Writing – review & editing, Validation, Project administration, Methodology, Formal analysis, Data curation. **Mohammad Hossein Khosravi:** Writing – review & editing, Validation, Supervision, Resources, Project administration, Investigation, Funding acquisition, Formal analysis, Conceptualization.

Data availability statement

The datasets and research materials associated with this study are available upon reasonable request.

Declaration of competing interest

The authors declare that they have no known competing financial interests or personal relationships that could have appeared to influence the work reported in this paper.

Acknowledgment

The authors would like to thank Mr. Mousa Poshtchi, for his valuable assistance with setup preparation and laboratory testing, and all the parties who assisted the authors in conducting this study.

List of Notations

The following symbols are used in this paper:

ξ	Included angle of the wedge
B	The tilt angle of the wedge
$\Delta\alpha$	The difference in dip direction of the slope face and discontinuities intersection line
K	Wedge factor
Ψ_{fi}	Apparent dip of the slope in the sliding direction
ψ_i	Dip angle of the discontinuities' intersection line
Φ	Friction angle
FS	Factor of safety
FS_W	Factor of safety of the wedge block
FS_P	Factor of safety of a cohesionless plane
P	Bulk density
Ω	Water content
W	Width of the wedge on each discontinuity plane
L	Length of the wedge
V_w	Volume of the wedge
Kn	Joint normal stiffness
Ks	Joint shear stiffness
G	Gravity vector

References

Ahmadi, M., Moosavi, M., Jafari, M.K., 2018. Experimental investigation of reverse fault rupture propagation through cohesive granular soils. Geomech. Energy Environ. 14, 61–65. https://doi.org/10.1016/j.gete.2018.04.004.

Ahmed, A., Ugai, K., Yang, Q.Q., 2012. Assessment of 3D slope stability analysis methods based on 3D simplified Janbu and hovland methods. Int. J. GeoMech. 12, 81–89. https://doi.org/10.1061/(ASCE)GM.1943-5622.0000117.

Alejano, L., González, J., Muralha, J., 2012. Comparison of different techniques of tilt testing and basic friction angle variability assessment. Rock Mech. Rock Eng. 45, 1023–1035. https://doi.org/10.1007/s00603-012-0265-7.

Alfat, S., Zulmasri, L.O.M., Asfar, S., Rianse, M.S., Eso, R., 2019. Slope stability analysis through variational slope geometry using Fellenius Method. In: Journal of Physics: Conference Series. IOP Publishing, p. 8. https://doi.org/10.1088/1742-6596/1242/1/012020.

Amini, E., Mojarab, M., Memarian, H., 2023. Identifying corresponding earthquake of Mobarak Abad landslide, Northeast Tehran, Iran. J. Min. Environ. 14, 1343–1359. https://doi.org/10.22044/jme.2023.13339.2453.

Amini, M., Ardestani, A., Khosravi, M.H., 2017. Stability analysis of slide-toe-toppling failure. Eng. Geol. 228, 82–96. https://doi.org/10.1016/j.enggeo.2017.07.008.

Amini, M., Golamzadeh, M., Khosravi, M.H., 2015. Physical and theoretical modeling of rock slopes against block-flexure toppling failure. Int. J. Min. Geol. Eng. 49, 155–171. https://doi.org/10.22059/ijmge.2015.56103.

Amini, M., Sarfaraz, H., Esmaeili, K., 2018. Stability analysis of slopes with a potential of slide-head-toppling failure. Int. J. Rock Mech. Min. Sci. 112, 108–121. https://doi.org/10.1016/j.ijrmms.2018.09.008.

BIOVIA, 2023. SOLIDWORKS, Release 2021, San Diego: Dassault Systems.

Bonilla-Sierra, V., Elmouttie, M., Donzé, F.-V., Scholtès, L., 2017. Composite wedge failure using photogrammetric measurements and DFN-DEM modelling. J. Rock Mech. Geotech. Eng. 9, 41–53. https://doi.org/10.1016/j.jrmge.2016.08.005.

Bowa, V.M., 2020. Wedge sliding analysis of the rock slope Subjected to Uplift forces and Surcharge Loads conditions. Geotech. Geol. Eng. 38, 367–374. https://doi.org/10.1007/s10706-019-01027-4.

Bowa, V.M., Kasanda, T., 2020. Wedge failure analyses of the jointed rock slope influenced by foliations. Geotech. Geol. Eng. 38, 4701–4710. https://doi.org/10.1007/s10706-020-01320-7.

Chen, Jie, Shi, K., Pu, Y., Apel, D.B., Zhang, C., Zuo, Y., Chen, Jiongkun, Xu, L., Gui, Z., Song, L., 2023. Study on instability fracture and simulation of surrounding rock induced by fault activation under mining influence. Rock Mech. Bull. 2, 9. https://doi.org/10.1016/j.rockmb.2023.100037.

Chen, Z., 2004. A generalized solution for tetrahedral rock wedge stability analysis. Int. J. Rock Mech. Min. Sci. 41, 613–628. https://doi.org/10.1016/j.ijrmms.2003.12.150.

Cundall, P.A., 1971. A computer model for simulating progressive, large-scale movement in blocky rock system. In: Proceedings of the International Symposium on Rock Mechanics, pp. 129–136.

Goodman, R.E., 1976. Methods of Geological Engineering in Discontinuous Rocks.

Hazari, S., Sharma, R.P., Ghosh, S., 2020. Swedish circle method for Pseudo-dynamic analysis of slope considering circular failure mechanism. Geotech. Geol. Eng. 38, 2573–2589. https://doi.org/10.1007/s10706-019-01170-y.

Hoek, E., Bray, J., 1981. Rock Slope Engineering, 3rd Edn, Inst. Mining and Metallurgy. London, UK.

Hoek, E., Bray, J.W., Boyd, J.M., 1973. The stability of a rock slope containing a wedge resting on two intersecting discontinuities. Q. J. Eng. Geol. 6, 1–55. https://doi.org/10.1144/GSL.QJEG.1973.006.01.01.

Jaiswal, A., Verma, A.K., Singh, T.N., 2024. Evaluation of slope stability through rock mass classification and kinematic analysis of some major slopes along NH-1A from Ramban to Banihal, North Western Himalayas. J. Rock Mech. Geotech. Eng. 16, 167–182. https://doi.org/10.1016/j.jrmge.2023.02.021.

Jiang, J.-C., Yamagami, T., 2004. Three-dimensional slope stability analysis using an extended Spencer method. Soils Found. 44, 127–135. https://doi.org/10.3208/sandf.44.4_127.

Jiang, Q., Liu, X., Wei, W., Zhou, C., 2013. A new method for analyzing the stability of rock wedges. Int. J. Rock Mech. Min. Sci. 60, 413–422. https://doi.org/10.1016/j.ijrmms.2013.01.008.

John, K.W., 1970. Engineering analyses of three-dimensional stability problems utilizing the reference hemisphere. In: Presented at the Proceedings of the 2nd International Congress of International Society on Rock Mechanics, OnePetro, pp. 314–321.

Khorasani, E., Amini, M., Hossaini, M.F., Medley, E., 2019. Statistical analysis of bimslope stability using physical and numerical models. Eng. Geol. 254, 13–24. https://doi.org/10.1016/j.enggeo.2019.03.023.

Khosravi, M.H., Pipatpongsa, T., Takahashi, A., Takemura, J., 2011. Arch action over an excavated pit on a stable scarp investigated by physical model tests. Soils Found. 51, 723–735. https://doi.org/10.3208/sandf.51.723.

Kim, D., Gratchev, I., Hein, M., Balasubramaniam, A., 2016. The application of normal stress reduction function in tilt tests for different block shapes. Rock Mech. Rock Eng. 49, 3041–3054. https://doi.org/10.1007/s00603-016-0989-x.

Kovári, K., Fritz, P., 1975. Stability analysis of rock slopes with plane and wedge failure by means of a pocket calculator. In: 16th U.S. Symposium on Rock Mechanics.

Kumar, S., Kumar, A., Rao, B., Choudhary, S.S., Burman, A., 2024. Analysis of 2D and 3D slope stability using the Bishop simplified method. In: IOP Conference Series: Earth and Environmental Science. IOP Publishing, p. 10. https://doi.org/10.1088/1755-1315/1326/1/012117.

Kumsar, H., Aydan, Ö., Ulusay, R., 2000. Dynamic and static stability assessment of rock slopes against wedge failures. Rock Mech. Rock Eng. 33, 31–51. https://doi.org/10.1007/s006030050003.

Li, X.Z., Jiang, H., Pan, Q.J., Zhao, L.H., 2023. Characterizing model uncertainty of upper-bound limit analysis on slopes using 3D rotational failure mechanism. Rock Mech. Bull. 2, 6. https://doi.org/10.1016/j.rockmb.2022.100026.

Ling, H.I., Wu, M.-H., Leshchinsky, D., Leshchinsky, B., 2009. Centrifuge modeling of slope instability. J. Geotech. Geoenviron. Eng. 135, 758–767. https://doi.org/10.1061/(ASCE)GT.1943-5606.0000024.

Lucas, J.M., 1980. A general stereographic method for determining the possible mode of failure of any tetrahedral rock wedge. Int. J. Rock Mech. Min. Sci. Geomech. Abstracts 17, 57–61. https://doi.org/10.1016/0148-9062(80)90006-6.

Mahmoodzadeh, A., Alanazi, A., Hussein Mohammed, A., Hashim Ibrahim, H., Alqahtani, A., Alsubai, S., Babeker Elhag, A., 2023. Comprehensive analysis of multiple machine learning techniques for rock slope failure prediction. J. Rock Mech. Geotech. Eng. https://doi.org/10.1016/j.jrmge.2023.08.023.

Moussaei, N., Khosravi, M.H., Hossaini, M.F., 2019. Physical modeling of tunnel induced displacement in sandy grounds. Tunn. Undergr. Space Technol. 90, 19–27. https://doi.org/10.1016/j.tust.2019.04.022.

Prabowo, H., Suryani, I., Sabilillah, I., 2024. Slope stability analysis at disposal mine area using Morgenstern price method. In: AIP Conference Proceedings. AIP Publishing. https://doi.org/10.1063/5.0184136.

Pradhan, S.P., Siddique, T., 2020. Stability assessment of landslide-prone road cut rock slopes in Himalayan terrain: a finite element method based approach. J. Rock Mech. Geotech. Eng. 12, 59–73. https://doi.org/10.1016/j.jrmge.2018.12.018.

Rabat, Á., Tomás, R., Cano, M., Pérez-Rey, I., Siles, J.S., Alejano, L.R., 2022. Influence of water content on the basic friction angle of porous limestones—experimental study using an automated tilting table. Bull. Eng. Geol. Environ. 81, 21. https://doi.org/10.1007/s10064-022-02687-y.

Sabermahani, M., Ghalandarzadeh, A., Fakher, A., 2009. Experimental study on seismic deformation modes of reinforced-soil walls. Geotext. Geomembranes 27, 121–136. https://doi.org/10.1016/j.geotexmem.2008.09.009.

Sarfaraz, H., Amini, E., Sarlak, M., Ashoor, F., 2023a. Determination of shear strength parameters using back analysis and comparing with physical and numerical modelings. J. Environ. Sustain. Min. 1, 69–78. https://doi.org/10.22111/jesm.2023.47077.1007.

Sarfaraz, H., Sarlak, M., Ashoor, F., Amini, E., 2023b. Block toppling stability of rock block with rounded edges using Sarma approach. J. Min. Environ. 14, 341–353. https://doi.org/10.22044/jme.2023.12630.2295.

Sheng, K., Hong, B.-N., Liu, X., Shan, H., 2021. Modified Bishop method for stability analysis of weakly sloped subgrade under centrifuge model test. Front. Struct. Civ. Eng. 15, 727–741. https://doi.org/10.1007/s11709-021-0730-z.

Singh, J., Verma, A.K., Banka, H., kumar, Ravishankar, Jaiswal, A., 2024. Optics-based metaheuristic approach to assess critical failure surfaces in both circular and non-circular failure modes for slope stability analysis. Rock Mech. Bull. 3, 18. https://doi.org/10.1016/j.rockmb.2023.100084.

Vaneghi, R.G., Saberhosseini, S.E., Dyskin, A.V., Thoeni, K., Sharifzadeh, M., Sarmadivaleh, M., 2021. Sources of variability in laboratory rock test results. J. Rock Mech. Geotech. Eng. 13, 985–1001. https://doi.org/10.1016/j.jrmge.2021.03.007.

Wang, H., Chen, Z., Zhang, D., 2012. Rock slope stability analysis based on FLAC3D numerical simulation. Appl. Mech. Mater. 170–173, 375–379. https://doi.org/10.4028/www.scientific.net/AMM.170-173.375.

Wang, Z., Jiang, L., Xia, Y., Pei, Y., Lin, M., 2014. Numerical analysis of stratified rock slope stability based on 3DEC. Appl. Mech. Mater. 454, 133–139. https://doi.org/10.4028/www.scientific.net/AMM.454.133.

Wittke, W., 1965. Methods to analyze the stability of rock slopes with and without additional loading. Rock Mech. Eng. Geol. 52–79.

Wu, C., Zhang, J., Zhou, M., Wang, L., 2023. Resistance factors for design of slopes in a homogenous soil layer. Rock Mech. Bull. 2, 10. https://doi.org/10.1016/j.rockmb.2022.100022.

Wyllie, D.C., Mah, C., 2004. Rock Slope Engineering, fourth ed. CRC Press.

Yang, X., Hu, J., Sun, H., Zheng, J., 2024. An approach for determination of lateral limit angle in kinematic planar sliding analysis for rock slopes. J. Rock Mech. Geotech. Eng. 16, 1305–1314. https://doi.org/10.1016/j.jrmge.2023.09.013.

Yoon, W.S., Jeong, U.J., Kim, J.H., 2002. Kinematic analysis for sliding failure of multi-faced rock slopes. Eng. Geol. 67, 51–61. https://doi.org/10.1016/S0013-7952(02)00144-8.

Zhao, T., Collins, P.E., 2024. Modelling the brittle rock failure by the quaternion-based bonded-particle model in DEM. Rock Mech. Bull. 3, 9. https://doi.org/10.1016/j.rockmb.2024.100115.

Zheng, J., Kulatilake, P., Deng, J., Wei, J., 2016. Development of a probabilistic kinematic wedge sliding analysis procedure and application to a rock slope at a hydropower site in China. Bull. Eng. Geol. Environ. 75, 1413–1428.

Zheng, J., Kulatilake, P.H.S.W., Shu, B., 2017. Improved probabilistic kinematic analysis procedure based on finite size discontinuities and its application to a rock slope at open pit mine in U.S. Int. J. GeoMech. 17, 15. https://doi.org/10.1061/(ASCE)GM.1943-5622.0000721.